

Measurement of $^{16}\text{O}(\gamma,n)^{15}\text{O}$ at Medium Energies

E. J. Beise,^(a) G. Dodson, M. Garçon,^(b) S. Høibråten,^(c) C. Maher,^(d) L. D. Pham, R. P. Redwine,
W. Sapp, K. E. Wilson, and S. A. Wood^(e)

*Bates Linear Accelerator Center, Laboratory for Nuclear Science, and Department of Physics,
Massachusetts Institute of Technology, Cambridge, Massachusetts 02139*

M. Deady

Department of Physics, Bard College, Annandale-on-Hudson, New York 12504

(Received 3 February 1989)

Exclusive differential cross sections for the $^{16}\text{O}(\gamma,n)^{15}\text{O}$ process have been measured for $E_\gamma=150$, 200, and 250 MeV and $\theta_L=49^\circ$, 59° , and 88° . This measurement is the first of its type to be reported for the energy region above the pion production threshold. An uncollimated bremsstrahlung beam was incident on an H_2O target, and neutrons were measured with a recoil-proton spectrometer with resolution sufficient to identify the residual ^{15}O ground state. The results are compared to (γ,p) data and to calculations including effects from meson exchange currents.

PACS numbers: 25.20.Dc, 27.20.+n

Exclusive (γ,N) reactions, where the residual nucleus is left in its ground state or a low-lying excited state, have traditionally been considered a probe of high-momentum components of the nuclear wave function. At intermediate photon energies (50–300 MeV), where there is a large (compared to the Fermi momentum) difference in momentum between the incoming photon and the outgoing nucleon, it is possible to reach higher nucleon momenta than are presently accessible through $(e,e'N)$ reactions and thus probe the kinematic region where short-range correlations are expected to be important. Below the pion production threshold, (γ,p) data^{1–5} on a variety of nuclei are explained reasonably well by a quasifree knockout (QFK) description.⁶ More recent tagged photon (γ,p) (Ref. 7) and (γ,pn) (Ref. 8) data on ^{12}C give evidence for contributions from two-body processes in addition to QFK. The (γ,n) data^{5,9–11} which exist in this energy region are underestimated by at least an order of magnitude, and some of the measured $^{16}\text{O}(\gamma,p)$ cross sections^{12,13} above 100 MeV are also much larger than predicted by the QFK description. The similarities in both the magnitude and shape of the existing (γ,p) and (γ,n) cross sections at lower energies suggest that two-body mechanisms may provide a better description. Several different approaches to this idea have been suggested. These include a simple quasideuteron calculation,^{5,14} self-consistent RPA calculations^{15,16} stressing long-range $N-N$ correlations, and calculations stressing the dominance of either nonresonant¹⁷ (meson exchange currents) or resonant¹⁸ (Δ production) pion exchange. All can qualitatively account for the similarities between (γ,p) and (γ,n) below 100 MeV. At higher energies these calculations at best predict the general behavior of (γ,p) (see Ref. 12). There is only one published quantitative prediction for (γ,n) above the pion production threshold¹⁷ and until now there have been no

(γ,n) data for $A > 4$ with which to make a comparison.

Presented here are results from an experiment at the Bates Linear Accelerator Center, in which (γ,n) cross sections on ^{16}O were measured at $E_\gamma=150$, 200, and 250 MeV and $\theta_L=49^\circ$, 59° , and 88° . In order to detect neutrons with sufficient energy resolution to resolve the ground state of ^{15}O a recoil-proton spectrometer was used. A detailed description of the spectrometer will be reported elsewhere;¹⁹ a brief description is presented here (see Fig. 1). Neutrons enter the spectrometer through a Pb filter, a small sweeping magnet (SWEEP), and two veto counters (V), and pass through ten plastic scintillator conversion planes (C1–10), where protons are produced from $p(n,p)n$ forward scattering. The protons are then momentum analyzed using two multiwire proportional chambers (MWPC) (WC1,2), a dipole magnet, and a set of rear detectors which consisted of two MWPC's (WC3,4) and two sets of three trigger scintillators (SA,SB). By tracing the proton trajectory back to the conversion point, using the MWPC information and the measured energy loss in the converter stack, one can both determine the (n,p) scattering angle and correct the measured proton momentum for losses in the converter stack. Thus the neutron energy and angle are known. The exclusive (γ,n) cross section for the transition to the residual ^{15}O ground state is then deduced from the number of neutrons in the top 5 MeV of the neutron energy spectrum.

The neutron energy resolution was estimated with a detailed Monte Carlo calculation to be 2% for the energy region of interest in the present experiment. The spectrometer momentum resolution was checked by measuring elastic electron scattering from ^{12}C (replacing the Pb filter with a small collimator) and was consistent with the Monte Carlo result. The pulse-height resolution in the converter stack was also verified by energy-loss cal-

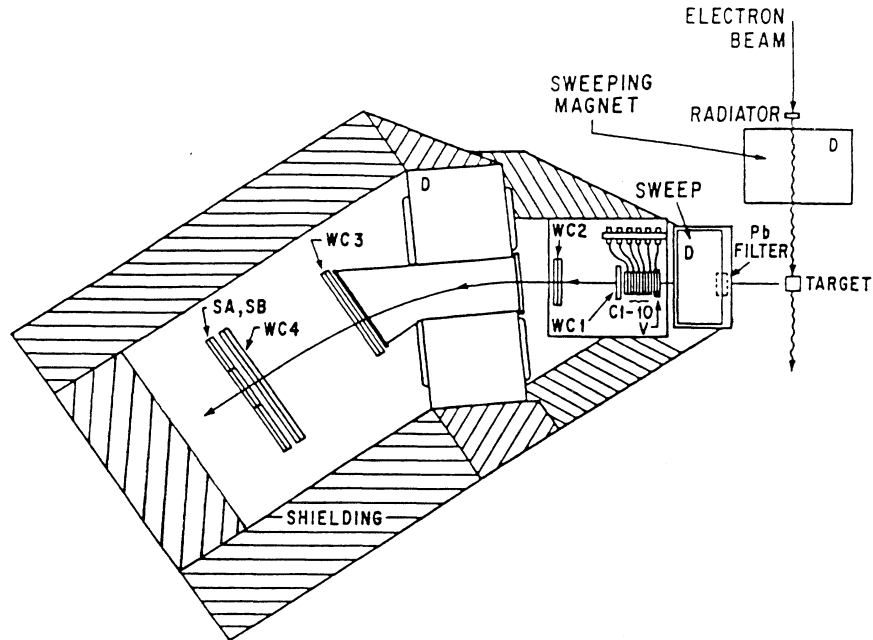


FIG. 1. Layout of the Bates recoil-proton spectrometer, as configured at the photon beam line.

culations and gives only a small contribution to the overall energy resolution. The efficiency-solid-angle product, also determined from the Monte Carlo calculation, was between 0.5 and 2.5×10^{-3} msr, depending on the setup for each angle. The efficiency was mainly determined by the forward-angle (n,p) differential cross section and the proton angular acceptance of the spectrometer, which was 12° . By limiting the proton angles to such a narrow range it was guaranteed that the highest-energy protons could have come only from H in the converter stack and not from ^{12}C .

The photon beam was from a tungsten radiator 0.04 radiation length thick placed in the electron beam 1 m upstream of the experimental target. The target was a plastic cell 10 by 10 cm^2 in area and 5 cm thick filled with H_2O . Between the target and radiator, the electron beam was deflected into a graphite dump approximately 7 m below beam height, shielded by 3 m of concrete. The bremsstrahlung beam continued uncollimated to the target and, because of the short target-to-radiator distance, was well contained within the target area. The typical photon flux of 2×10^{10} photons/sec in the top 5 MeV was limited by the singles rates in the front wire chambers and in the converter stack. The dominant source of background came directly from the target, and was mainly neutrons produced by lower-energy photons.

The largest source of contamination in the measured neutron energy spectrum was fast deuterons generated by pickup reactions in ^{12}C in the converter stack. It was possible to identify the mass of the particle creating a good track in the spectrometer by reconstruction of the flight time, based on the timing information from the

converters at the front and the rear trigger scintillators. Once the forward deuteron events were removed from the reconstructed neutron kinetic energy spectrum, an end point could be seen clearly with no high-energy

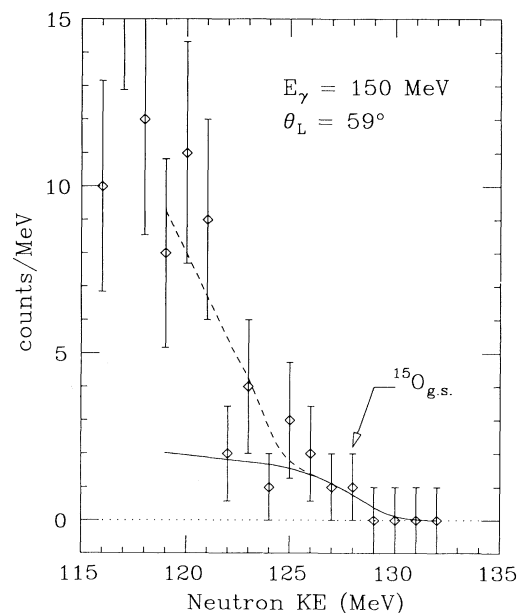


FIG. 2. A neutron end-point energy spectrum observed in the $^{16}\text{O}(\gamma,n)^{15}\text{O}$ experiment. The solid line represents a fit to the cross section of the transition to the ground state of ^{15}O using a theoretical bremsstrahlung spectrum. The dashed line includes a fit to an excited state at 6 MeV, where the $\frac{3}{2}^-$ state is expected.

background. Cross sections were then extracted by fitting the end-point region with a theoretical bremsstrahlung spectrum,²⁰ similar to the analysis procedure described in Ref. 12. A typical fitted end-point spectrum is shown in Fig. 2. Given the statistics of the data, only the ground-state cross sections could be extracted with any precision. It is in any event not sensible to try to use data below the top 10 MeV because below this point one can no longer guarantee that the recoil protons contributing to the spectrum came from a $p(n,p)n$ reaction.

Figure 3 contains the extracted laboratory cross sections, compared to available (γ,p) data^{12,13,21} and plotted versus the momentum mismatch, $p_m = |\mathbf{p}_N - \mathbf{k}_\gamma|$. In a simple QFK picture this is just the initial momentum of the struck nucleon. The error bars on the data are statistical only. The systematic error in the cross section was due mostly to the 1% uncertainty in the absolute calibration of the spectrometer and in the electron beam energy; it is estimated to be 30%. Two interesting features to note in this figure are, first, that the (γ,n) and (γ,p) data are quite similar at the lowest energy, and second, that there is a systematic increase in (γ,n) compared to (γ,p) as the photon energy increases into the region of Δ production.

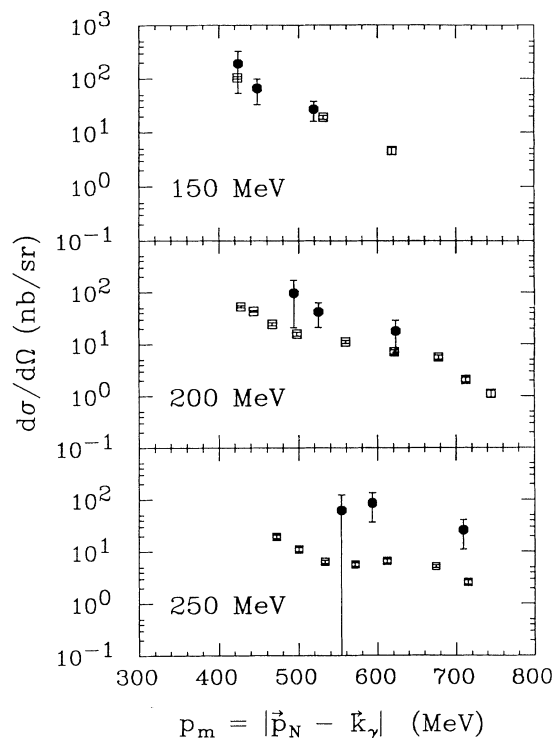


FIG. 3. Laboratory cross sections (solid circles) for the $^{16}\text{O}(\gamma,n)^{15}\text{O}$ reaction, compared to (γ,p) (open squares) as a function of momentum mismatch (see text). The (γ,p) data are from, 150 MeV, Ref. 12; 200 MeV, Ref. 13, 250 MeV, Ref. 21.

The only calculation which has yielded detailed predictions for (γ,n) is that of Gari and Hebach,¹⁷ in which it is suggested that the major contribution to the cross section comes from nonresonant meson exchange currents. At higher energies and some angles the calculated cross section is larger for (γ,n) than for (γ,p) , because the large QFK term in (γ,p) can interfere with other effects. This calculation has been criticized by some authors² for using a rather unrealistic single-particle potential in order to maintain orthogonality between initial and final states of the ejected nucleon, the effect of which is to underestimate the contribution of quasifree knockout. Since the QFK term is relatively unimportant for (γ,n) , such an approximation may be justified. Gari and Hebach do not include any contribution from production of the Δ resonance in the (γ,n) calculation, since they estimate its effects to be small at forward angles in (γ,p) compared to nonresonant meson exchange. Even if the effects of Δ production are small in (γ,p) , it is possible that one could see a large contribution from the Δ in the (γ,n) cross section above 200 MeV.

The comparisons between Gari and Hebach's calculation, various other calculations, and the (γ,p) data have been discussed at length in Ref. 12. There, the authors concluded that given the current state of both calculation and experiment it is difficult to make any statement about the dominance of a particular reaction mechanism in the (γ,N) process. As more detailed angular distributions of $^{16}\text{O}(\gamma,p)$ have become available,^{13,21} more theoretical work^{16,22,23} on both (γ,p) and (γ,n) is also

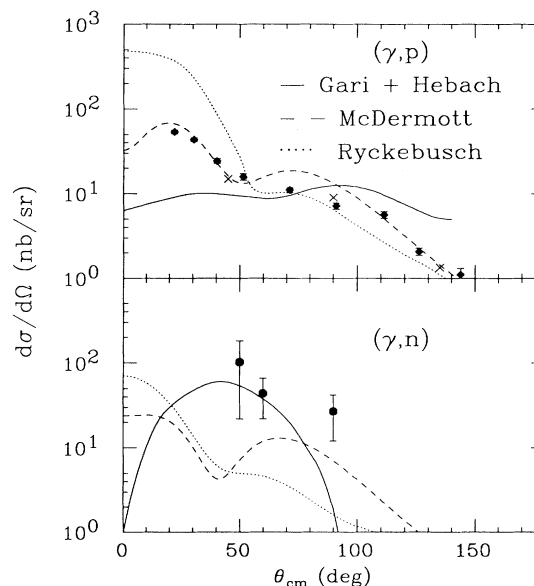


FIG. 4. Angular distributions of (γ,p) and (γ,n) at 200 MeV, compared to three different calculations (Refs. 16, 17, and 22). The (γ,n) calculations of both McDermott *et al.* and Rycebusch *et al.* are preliminary.

under way. These newer calculations have taken the approach that one should first understand QFK before attempting to evaluate the contributions from other reaction mechanisms, and so far the results for (γ, p) have been quite promising, as can be seen in Fig. 4. Comparisons to the first results for (γ, n) are somewhat less convincing. However, the contribution to (γ, n) from single-particle knockout must be small, which makes the (γ, n) process more sensitive to other reaction mechanisms, such as meson exchange and Δ production, which cannot be unambiguously determined in (γ, p) .

The difficulty of detecting neutrons with good resolution at medium energies has until now made direct comparisons between the knockout of neutrons and protons in this energy range impossible in all but the lightest nuclei.²⁴ The present experiment has not only provided the first report of (γ, n) data on any nucleus except ⁴He above the pion production threshold, but has also shown that such measurements can be performed with present-day techniques. An important limitation on the precision of the data presented here has been statistical, resulting from a necessarily low beam current in order to keep singles rates in the front detectors at a reasonable level. The planned increase in the duty factor of the Bates accelerator to 100% would allow a significant increase in the data rate, resulting in a substantial improvement in such measurements.

This work was supported under DOE Contract No. DE-AC02-76ER03069. The authors would like to thank J. Ryckebusch and J. McDermott for allowing their calculations to be shown prior to publication. We would also like to thank the Bates mechanical and research support staff for their efforts both before and during the running of this experiment.

^(a)Present address: Kellogg Radiation Laboratory, Caltech, Pasadena, CA 91125.

^(b)On leave from Département de Physique Nucléaire-Moyenne Energie, Centre d'Etudes Nucléaires de Saclay, 91191 Gif-Sur-Yvette CEDEX, France.

^(c)Present address: Nuclear Physics Laboratory, University of Colorado, Boulder, CO 80309-0446.

^(d)Present address: Carnegie-Mellon University, Pittsburgh, PA 15213.

^(e)Present address: University of Illinois, Urbana, IL 61801.

¹J. L. Matthews *et al.*, Nucl. Phys. **A267**, 51 (1976).

²D. J. S. Findlay and R. O. Owens, Nucl. Phys. **A279**, 385 (1977).

³D. J. S. Findlay, D. J. Gibson, R. O. Owens, and J. L. Matthews, Phys. Lett. **79B**, 356 (1978).

⁴A. C. Shotton *et al.*, Phys. Rev. C **37**, 1354 (1988).

⁵M. R. Sené *et al.*, Nucl. Phys. **A442**, 215 (1985); M. R. Sené *et al.*, Phys. Rev. Lett. **50**, 1831 (1983).

⁶S. Boffi, C. Guisti, and F. Pacati, Nucl. Phys. **A359**, 91 (1981).

⁷J. C. McGeorge *et al.*, Phys. Lett. **B 179**, 212 (1986).

⁸S. N. Dancer *et al.*, Phys. Rev. Lett. **61**, 1170 (1988).

⁹H. Schier and B. Schoch, Nucl. Phys. **A229**, 93 (1974).

¹⁰B. Schoch and H. Göringer, Phys. Lett. **109B**, 11 (1982).

¹¹P. D. Harty *et al.*, Phys. Rev. C **37**, 13 (1988).

¹²M. Leitch *et al.*, Phys. Rev. C **31**, 1633 (1985).

¹³S. Turley *et al.*, Phys. Lett. **157B**, 19 (1985).

¹⁴B. Schoch, Phys. Rev. Lett. **41**, 80 (1978); Habilitationsschrift, Universität Mainz, 1980 (unpublished).

¹⁵M. Cavinato, M. Marangoni, and A. M. Saruis, Nucl. Phys. **A422**, 237 (1984).

¹⁶J. Ryckebusch *et al.*, Nucl. Phys. **A476**, 237 (1988); J. Ryckebusch (private communication).

¹⁷H. Hebach, A. Wortberg, and M. Gari, Nucl. Phys. **A267**, 425 (1976); M. Gari and H. Hebach, Phys. Rep. **72**, 1 (1981).

¹⁸J. T. Londergan and G. D. Nixon, Phys. Rev. C **19**, 998 (1979).

¹⁹E. J. Beise *et al.* (to be published).

²⁰J. L. Matthews and R. O. Owens, Nucl. Instrum. Methods **180**, 157 (1973).

²¹G. Adams *et al.*, Phys. Rev. C **38**, 2771 (1988).

²²J. P. McDermott *et al.*, Phys. Rev. Lett. **61**, 814 (1988); (private communication).

²³G. M. Lotz and H. S. Sherif, Phys. Lett. **B 210**, 45 (1988).

²⁴R. Schumacher *et al.*, Phys. Rev. C **33**, 50 (1986).